Wet and Dry Regions in Jupiter's Atmosphere

M. Roos-Serote*, A.R. Vasavada†, L. Kamp‡, P. Drossart§, P. Irwin||, C. Nixon||,

& R.W. Carlson‡.

* Observatório Astronómico de Lisboa, Tapada da Ajuda, 1349–018 Lisbon, Portugal

† Department of Earth and Space Sciences, University of California at Los Angeles,

Los Angeles, California 90095, USA

‡ Jet Propulsion Laboratory, California Institute of Technology, 4800 Oak Grove Drive,

Pasadena, California 91109, USA

§ Département Spatial (CNRS–UMR8632), Observatoire de Paris–Meudon,

5, Place Janssen, 92915 Meudon Cedex, France

|| Atmospheric Physics Department, Clarendon Laboratory, Oxford University,

Parksroad, Oxford OX13PU, United Kingdom

Submitted to *Nature*, October 1999

Revised December 1999

Models of Jupiter's formation and interior predict that its atmosphere is enriched in oxygen relative to the Sun and that consequently, a water cloud is present globally near the 5–bar pressure level[1,2]. The water vapour abundance and vertical cloud structure in the troposphere can be inferred[3] from observations at wavelengths near 5 μm. However, past attempts have led to contradictory results[4,5,6]. The *in situ* measurements by the Galileo probe revealed a very dry atmosphere at the entry site with no significant clouds below 2 bars[7,8]. Data from instruments on the Galileo orbiter agree in most cases with the *in situ* measurements[9,10]. While the entry site was known to be a relatively cloud–free region on the planet, the contrast between the local conditions and those thought to represent Jupiter in a global sense was surprising. Here we report an analysis of Galileo near–infrared data that for the first time reveals extreme spatial variations in relative humidity and their correlation with visible cloud systems. These findings underscore the complex distribution and role of jovian water and its interdependence on local meteorology, including moist convection.

During Galileo's fourth orbit (E4) in December 1996, the Near Infrared Mapping Spectrometer (NIMS) and the Solid State Imager (SSI) on the Galileo spacecraft acquired data over the same region of Jupiter's atmosphere within a time span of 64 hours. The region contained a "5–μm hot spot", a relatively cloud-free area where thermal radiation from the deep atmosphere escapes to space, and an evolving, bright cloud northward of it (Figure 1). The low spectral resolving power (200) of the NIMS instrument and the weakness of the 5–μm water absorption bands preclude the direct retrieval of the deep water abundance. However, the integrated column density of water between about 3 and 8 bar can be retrieved. The depth of the water band at 5.025 μm, D, defined as the difference between the radiance at the continuum (out–of–band) wavelength (5.052 μm) and the center of the water band (5.025 μm) divided by the continuum radiance, is a proxy for the amount of water vapour in this part of the troposphere. We modelled it as the relative humidity, RH, which is actual normalized to the saturated water vapour pressure at the ambient temperature. Model calculations indicate that D varies between about 0.23 for dry spectra ($RH = \sim$1%) and 0.4 for very wet spectra ($RH >\sim$20%).

In order to assess the relative humidity and cloud structure within and surrounding the hot spot, we modelled NIMS spectra using a line–by–line (LBL) radiative transfer code. The cloud scattering was simplified by replacing cloud layers with absorbing/reflecting layers[9]. Model 1 has one cloud layer at 1.55 bar, similar to the Galileo probe observations[8], whereas model 2 includes an additional opacity source (the water cloud) at 5.6 bars, similar to Carlson *et al.* (1992)[6]. In addition, a correlated-k code including multiple scattering[10] was employed to confirm its validity, with one cloud layer at 1.55 bar (model 3). The atmospheric thermal structure is taken from Galileo probe *in situ* measurements. Cases

were run assuming a range of RH and two models of vertical cloud structure.

Model 1 produces a good fit to hot spot spectra for RH $<\sim$1%. Model 2, which includes the 5.6–bar cloud, produces a poor fit and rules out the existence of a deep cloud within the hot spot (Figure 2). Outside of the hot spot, both models produce similarly good fits. However, in all cases, model 2 requires a much greater RH than model 1. This non-uniqueness can be understood when studying the contribution functions (CF), the kernel of the radiative transfer integral. For small values of RH, the CFs peak near 6 bars, so a cloud layer at 5.6 bars strongly affects the shape of spectra measured from orbit[11] (Figure 2). When RH $>\sim$20%, the greatest contribution is from above the 5.6–bar level, so that the shape of the spectrum is not much affected by the presence of an opacity layer at this level. The effects of opacity at 5.6 bars are to "cut off" contribution to the outcoming radiation from below this level, and thus require a higher water vapour concentration above this level in order to still fit the water band depth. Because it is not possible to unambiguously detect the presence of a water cloud in this region, the RH from Model 1 should be taken as a lower limit.

Our primary finding is that extremely dry regions, such as the E4 hotspot with RH between 0.1% and 1%, exist in close proximity to wet areas, characterized by RH $>\sim$ 20%. The presence of a deep water cloud is excluded in the dry regions. While the precision of derived water vapour mixing ratios is limited by model assumptions, the above analysis shows that relatively dry and wet areas are easily distinguished using the observed 5.025–μm water band depth. Inside the hot spot the water band is shallow (D = 0.2 - 0.28), while outside the hot spot it is generally deeper (D = 0.3 - 0.33). At other locations it is very deep (D = 0.33 - 0.4). Clearly local meteorology creates a more complex distribution

of relative humidity than expected solely from thermodynamical models[1,2].

Images at visible and near-infrared wavelengths from the SSI yield some insight into the local dynamics and cloud structure down to about 3 bars. Banfield *et al.*[12] first noted the vertical extension of small ($\sim 10^3$ km horizontal), bright clouds and conjectured that they are convective towers stemming from the jovian water cloud. The E4 bright cloud lies in a cyclonic shear zone, where the horizontal zonal flow is changing direction from about 100 ms^{-1} eastward at 6°N to about 25 ms^{-1} westward at 15°N[13]. Cyclonic shear zones on Jupiter are characterized by chaotic cloud systems, outbursts of bright cloud material, and from recent Galileo results, the occurence of lightning[14,15]. Using SSI images, Gierasch *et al.*[16] found deep (>3 bars) clouds in the area surrounding the E4 bright cloud. When this cloud's position is corrected for wind advection, it coincides with a NIMS wet area (Figure 1). Our spectroscopic results greatly strengthen the case that the deep clouds are indeed convecting water clouds which result in lightning and the formation of bright cloud material at higher altitudes. These widespread and energetic convection events may be a dominant source of energy for driving Jupiter's winds[17].

NIMS has observed low relative humidity within a hot spot similar to the Galileo probe entry site and high humidities near a small, bright cloud similar to those thought to represent localized moist convective events[15]. Because NIMS measurements sound to deeper levels ($\sim$ 6 bar) than the bright clouds detected with SSI ($\sim$3 bar), some of the high-humidity regions may represent deeper clouds not apparent in the SSI data. Future joint investigations at visible and infrared wavelengths will best reveal phenomena related to the water cloud and moist convection and will help extend this work to global scale.

Correspondence and requests for materials should be addressed to

Maarten Roos-Serote

Observatório Astronómico de Lisboa

Tapada da Ajuda

1349-018 Lisboa

Portugal

email: roos@oal.ul.pt

References

1. Weidenschilling, S.J. & Lewis, J.S., Atmospheric and cloud structure of the jovian planets. *Icarus* **20**, 465–476 (1973).

2. Atreya, S.K. *et al.*, A comparison of the atmospheres of Jupiter and Saturn: deep atmospheric composition, cloud structure, vertical mixing, and origin. *Planet. Space Sci.* **47**, 1243–1262 (1999).

3. Larson, H.P, Fink, U., Treffers, R., & Gautier, T.N., Detection of water vapor on Jupiter. *Astrophys. J.* **197**, L137–L140 (1975).

4. Drossart, P., & Encrenaz Th., The abundance of water on Jupiter from the Voyager IRIS data at 5 microns. *Icarus* **52**, 483–491 (1982).

5. Bjoraker, G., Larson, H.P., & Kunde, V., The abundance and distribution of water vapor in Jupiter's atmosphere. *Astrophys. J.* **311**, 1058–1072 (1986).

6. Carlson, B.E., Lacis, A.A., & Rossow W.B., The abundance and distribution of water vaor in the jovian troposphere as inferred from Voyager IRIS observations. *Astrophys. J.* **388**. 648–668 (1992).

7. Niemann, H.B., *et al.*, The composition of the jovian atmosphere as determined by the Galileo probe mass spectrometer. *J. Geophys. Res.* **103**, 22,831–22,845 (1998).

8. Ragent, B., *et al.*, The clouds on Jupiter: results on the Galileo Jupiter mission probe nephelometer experiment. *J. Geophys. Res.* **103**, 22,891–22,910 (1998).

9. Roos–Serote, M., *et al.*, Analysis of Jupiter North Equatoral Belt hot spots in the 4–5 μm range from Galileo/near–infrared mapping spectrometer observations: measurements of cloud opacity, water and ammonia. *J. Geophys. Res.*, **103**, 23,023–23,041 (1998).

10. Irwin, P.,*et al.*, Cloud structure and atmospheric composition of Jupiter retreived

from Galileo near-infrared mapping spectrometer real–time spectra. *J. Geophys. Res.* **103**, 23,001–23,022 (1998).

11. Roos–Serote, M., Drossart, P., Encrenaz, Th., Carlson, R.W., & Leader, F., Constraints on the tropospheric cloud structure of Jupiter from spectroscopy in the 5–μm region: a comparison between Voyager/IRIS, Galileo/NIMS, and ISO/SWS spectra. *Icarus* **137**, 315–340 (1999).

12. Banfield, D. *et al.*, Jupiter's cloud structure from Galileo imaging data. *Icarus* **135**,230–250 (1998).

13. Limaye, S.S., Jupiter: New estimates of the mean zonal flow at the cloud level. *Icarus* **65**, 335–352 (1986).

14. Little, B., *et al.*, Galileo images of lightning on Jupiter. *Icarus* in press.

15. Gierasch, P. *et al.*, Moist convection observed on Jupiter by Galileo imaging. *To be published in Nature* (1999).

16. Gierasch, P. *et al.*, Cloud structure near convective locations on Jupiter. *B.A.A.S.* **31, no.4**, 1151 (1999).

17. Ingersoll, A.P., *et al.*, Moist convection as an energy source for large scale motions in Jupiter's atmosphere. *To be published in Nature* (1999).

18. Drossart, P., *et al.*, The solar reflected component in Jupiter's 5–μm spectra from NIMS/Galileo observations. *J. Geophys. Res.* **103**, 23,043–23,050 (1998).

19. Vasavada, A.R., *et al.*, Galileo imaging of Jupiter's atmosphere: The Great Red Spot, equatorial region, and white ovals. *Icarus* **135**, 265–275 (1998).

Acknowledgements

This work was partly performed at the Jet Propulsion Laboratory, California Institute of Technology, under contract with NASA, through the Jupiter System Data Analysis Program and the Galileo Project. M. Roos–Serote acknowledges financial support from PRAXIS XXI/FCT, and the French Embassy/ICCTI, Portugal. We thank Peter Gierasch, Don Banfield, and Thérèse Encrenaz for very constructive discussions, and Jan Yoshimizu for help in making the figure 1. Helpful comments were received from two anonymous referees.

Figure Captions

Figure 1:

Comparison between data from the Solid State Imager (SSI), the Near Infrared Mapping Spectrometer (NIMS) and model results.

(a) SSI images acquired using the 0.756 μm continuum filter on December 17^{th} 1996 at 17:13 UT (spatial resolution 30 km/pixel). A cloud system with high bright clouds at 329°.9 W and 10°.3 N can be identified (black cross).

(b) NIMS image at 5.052 μm taken on the night side of the planet on December 20^{th} 1996 at 09:06 UT (spatial resolution 640 km/pixel). The units on the color bar give radiance in μW cm^{-2} ster^{-1} μm^{-1}. The shape of the hot spot (dark in the visible and bright at 5 micron) did not change significantly in the 64 hours between the reflected sunlight and thermal observations. The positions of features visible in Figure 1a can be calculated using the zonal velocities derived from a set of SSI images spanning 11 hours[19]. The bright cloud has an eastward (to the right) velocity of $\approx$ 40 ms^{-1}. When the NIMS thermal data were acquired, the center of the bright cloud system is expected to be between 322°.5 and 320.°9 W (System III) and 10°.4 N (square).

(c) Map of the relative humidity derived from the NIMS 5–μm spectra from December 20^{th} 1996. The units on the color bar give relative humidity in percentage. High relative humidities are required to fit spectra from the region near the predicted location of the bright cloud (Figure 2).

(d) Map of 1.55-bar cloud opacities derived from the NIMS 5 micron spectra. The units on the color bar give the optical depth of the cloud at 1.55 bar. High cloud opacities are derived in the wet area, consistent with the SSI observations of a thick cloud deck.

Figure 2:

The 5–μm window of the jovian spectrum is free from strong absorptions of methane and ammonia. Radiation comes from 3 bar at 5.1 μm down to 8 bar at 4.65 μm. The overall continuum level is also sensitive to the total amount of cloud opacity above 2 bar. At NIMS spectral resolution, water dominates the absorption for wavelengths longer than 4.95 μm. At smaller wavelengths, phosphine dominates[9,10].

(a) Measured spectrum in the hot spot. The observed spectrum (solid line) was acquired at 319.2°W (System III) and 7.3°N and the 5.052–μm water band depth is 0.24. The values of the derived relative humidity and cloud optical depth (clouds above the 2 bar level) are listed for model 1 and 2. Only model 1 gives a good fit the spectrum. Model 2, including an opaque cloud at 5.6 bar, retrieves higher water abundances, as explained in the text.

(b) Measured spectrum of a wet region. The observed spectrum (solid line) was acquired at 320.8°W (System III) and 11°N and the 5.052–μm water band depth is 0.34. All models (described in the text) provide good fits to the spectrum. The fact that model 3 gives similar results as model 1 for the RH, confirms the validity of the non–scattering approximations applied in models 1 and 2. The difference in the estimated cloud opacities is due to the highly forward scattering particles of the 1.55 bar cloud in model 3, in contrast with the purely absorbing layer in model 1.

The NIMS spectra have a noise level of about 5 % on the radiance. This results in uncertainties of about 0.5 in the cloud opacity for opacities larger than 1, and a factor of about 3 for the relative humidity (models 1 and 2).

Figure 1.

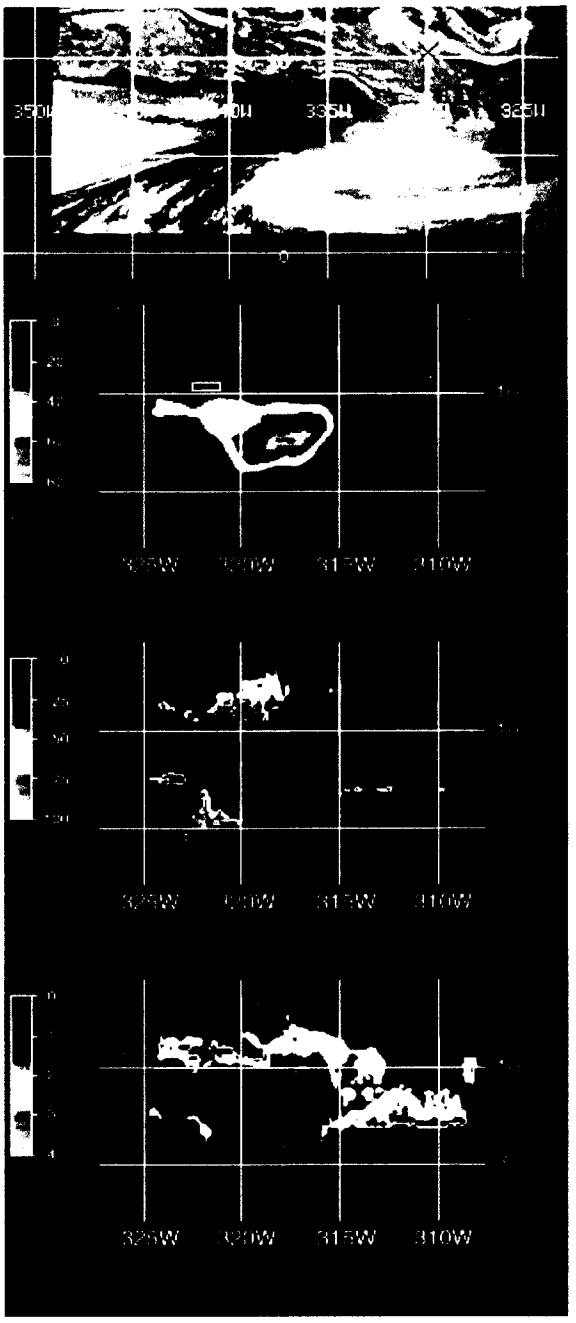

Figure 2

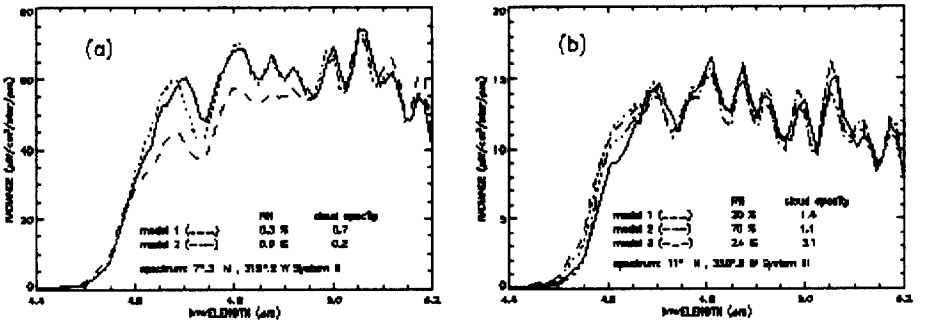
(a)
(b)